Section A-Research paper

SYNTHESIS, STRUCTURAL AND ANTI-MICROBIAL APPLICATION OF IRONOXIDE/CHITOSAN/CURCUMIN COATED NANOPARTICLES

N. Nasrin Farsana[1], M. Sheik MuhideenBadhusha[2], J.Shakina[3], M. Mohamed Roshan[4]

[1]Research Scholar, Sarah Tucker College, Tirunelveli-627 011
[2]Assistant Professor, Sadakathullah Appa College, Tirunelveli-627 011
[3]Assistant Professor, Sarah Tucker College, Palayamkottai, Tirunelveli-627 007
[4]Assistant Professor, Sadakathullah Appa College, Tirunelveli-627 011
(Affiliated to Manonmaniam Sundaranar University, Tirunelveli), Tirunelveli- 627 412)
doi: 10.48047/ecb/2023.12.si4.1026

ABSTRACT

Iron oxide nanoparticles are now widely used in biomedical applications because they are non-toxic to biological systems. Iron oxide nanoparticles' magnetic and semiconductor capabilities can also lead to multiple medical applications. The antibacterial, antifungal, and anticancer properties of these nanoparticles have been employed in the medical field. The diagnosis of cancer has been improved with the use of medicines and iron oxide nanoparticles for treatment. However, a lot of these medications have negative health impacts. As an alternative, plant-derived phytochemicals have been administered to functionalize these nanoparticles in order to counteract any unfavourable effects. In the present study, ex-situ co-precipitation was used to produce Fe_3O_4 nanoparticles that were then coated with Chitosan. Iron ferric and ferrous solutions were dissolved in ammonia to create Fe_3O_4 nanoparticles. Fe_3O_4 was synthesized prior to the addition of Chitosan. By using XRD, FTIR, SEM, UV-Vis methods, thermal (TGA) and magnetic (VSM) properties of nanoparticles with drug-loaded curcumin were identified.Then the samples' anti-microbial activities are determined by using the gram positive and gram negative bacteria. The results clearly prove the structural, strength and anti-microbial activity of ironoxide/chitosan/curcumin loaded nanoparticlesHence, thisnanoparticlescan be used as a drug in near future.

Keywords: Chitosan, iron-oxide nanoparticle, FT-IR, SEM, XRD, TGA, VSM and anti-microbial activity

INTRODUCTION

Nanoparticles constitute a fascinating topic for further research due to their distinctive properties. Recently, scientists have shown that nanoparticles can function at the cellular and molecular levels. They have been created for a variety of application areas. Different processes, including microemulsion, thermal breakdown, hydrothermal synthesis and co-precipitation, are used to synthesize them. The co-precipitation approach is popular since it is economical and it does not require heat, or a dangerous solvent.

Both organic (polymer) and inorganic (metal) materials can be used to create nanoparticles, according to Hariani et al. (2013). Chemotherapy is inappropriate for several treatments due to its significant side effects. Drugs affect more than just cells when they enter the body. As a result, magnetic particles can transport the medications to the target organ, or to the tissues, generally cancer tissues, in the body.

Because they are designed to be multifunctional and act as imaging contrast agents, therapeutic agents, and drug delivery vehicles simultaneously, nanoparticles are appealing for

use in cancer treatments. The impact of nanoparticles on safety and health has also been receiving increasing attention [Thacharodi et al., 1993]. Depending on their size, nanoparticles can infiltrate different types of target cells. Researchers have demonstrated that nanoparticles may enter cancer cells with ease. While several metal nanoparticles showed cytotoxicity after coming into contact with cells, iron oxide nanoparticles did not show cytotoxicity at lower doses (10–50 g/mL), but did show cytotoxicity at higher doses (100–250 g/mL) and interacted with cell components. Therefore, those nanoparticles may serve as a reliable method of medication administration and present fresh ideas for cancer diagnosis and treatment. The remarkable biocompatibility of magnetic particles like Fe_2O_3 nanoparticles allow for usage in vitro and in vivo applications such as resonance imaging.

Drugs are enclosed in biocompatible magnetic nanoparticles. They perform the role of drug delivery transporters and manage the drug release procedure. Consequently, the use of super-paramagnetic iron oxide nanoparticles in diagnostic and therapy has led to numerous promising successes, including cell separation [Chen et al., 2006], cell apoptosis, and enzyme immobilization. The drug-particle system creates a magnetic liquid that travels through the circulatory system to enter the body. A powerful external magnetic flux gradient is used when the particles enter the vessel to direct them toward the intended destination within the body. The drug release mechanism is initiated by enzyme activity, or a change in the physical characteristics of cancer cells that result in a change in pH, diffusion, and temperature when the drug-particle system is concentrated at the designated area. Magnetism makes it simple to target the medicine carried by magnetic nanoparticles to a specific area within the body. Drugs with polymer coatings may respond more slowly. The magnetic nanoparticle coated polymer systems are therefore regarded as an effective way to target tumour cells specifically.

Researchers have recently paid a great deal of attention to the production of oxide nanoparticles of homogenous size due to their distinctive optical, electrical, and magnetic properties and their potential use in a variety of biomedical applications. Hematite (α-Fe_2O_3), maghemite (γ-Fe_2O_3), and magnetite (Fe_3O_4) are three different types of iron oxides that are classified as significant materials. Hematite (α-Fe_2O_3) is a thermodynamically stable iron oxide among them when found in natural environments. It has a corundum structure and it gives a high level of corrosion resistance. It is the most environmentally benign n-type semiconductor material due to its low cost and lack of toxicity (band gap of 2.1 eV)

The particle-size, morphology and structure of α-Fe_2O_3 have a significant impact on its characteristics. Several methods, including thermal oxidation, hydrothermal processing, mechanical milling, microwave synthesis and sol-gel, are developed to produce nanostructures of α- Fe_2O_3 powder. Sol-gel combustion is a low-cost technology that offers a straightforward production process. Magnetic nanoparticles have the potential to be useful tools in a range of medicinal applications such as drug delivery in chemotherapy for cancer.

Deacetylated chitin, which is used to make Chitosan, is both biocompatible and biodegradable. As a result, it can be utilized in a medication delivery system combined with magnetic (Fe_3O_4) nanoparticles. Chitosan is most stable in the neutral state and is least stable when the pH is 6.5. The Crosslinker method is used to create Chitosan nanoparticles. Crosslinker has also helped to keep Chitosan stable under acidic conditions. Chitosan will break down when the pH of a tumor cell is around 5.5 if the Crosslinker agent is not employed. Drug release will therefore happen soon. To prevent Chitosan from degrading and to regulate the release of drugs from the Chitosan-Fe_3O_4 nanoparticle structure, a cross-linking agent is used (Unsoy et al., 2012). Natural Chitosan, one of the available polymers, exhibits some promising outcomes as a drug delivery mechanism. Chitosan (CS), a naturally occurring bio-polymer produced by alkaline deacetylation of chitin, is the second most prevalent polymer in nature after cellulose. The chemical structure of CS has attracted a lot of

attention because of its benign properties (Muzzarelli et al., 1999) and a variety of applications, including adsorbent and anti-bacterial membrane. In several contemporary applications, CS is frequently used in protein carriers and medication delivery systems.

The anti-cancer medication curcumin is made from phenol, which is joined by two unsaturated carbonyl groups. The diketones quickly deprotonate to create enolates and form stable enols. The unsaturated carbonyl group underwent nucleophilic addition and is an excellent michael acceptor. As a result, they are biologically classified as having antioxidant, anti-inflammatory, antibacterial (Kawamori et al., 1999) and anticancer action (Aggarwal et al., 2007 and Mahady et al., 2002).

Materials and Procedures

Magnetic Fe_3O_4 nanoparticle synthesis

The water-in-oil micro-emulsion process heavily utilizes Fe_3O_4. 45 ml of a mixture of tween-80, butan-1-ol, and n-heptane dissolve the solution A, which contains a 2:1 mole proportion of iron salts. 45 ml of tween-80/butan-1-ol/n-heptane were added to fluid NH3 to create Solution B. These mixtures were stirred for 30 minutes at room temperature at a speed of 300 rpm. Micro-emulsion was combined with Blend B, and the resulting mixture was continuously mixed for 24 hours at various temperatures of 30, 50, and 80 °C. The created nanoparticles were then separated by attractive force and repeatedly rinsed with purified water to remove the smelly salts. Following drying in a vacuum stove, the alluring Fe_3O_4 nanoparticles were obtained and identified as Fe_3O_4-30, Fe_3O_4-50, and Fe_3O_4-80, respectively.

Chitosan-coated magnetic Fe_3O_4 nanoparticle synthesis (MNPs)

The method employed to create the Chitosan-coated magnetic iron oxide nanoparticles was suspension Cross-linking. In this particular procedure, a 2 percent aqueous acetic acid solution (10 ml acetic acid in 500 ml deionized water) containing 1 g Fe_3O_4 dry magnetic nanoparticles was used to prepare a 5 percent Chitosan (25 grams) solution. This solution was then dropped one at a time into the dispersion medium, which was made up of 140 ml paraffin and 2.5 ml span-80. The dispersion media was agitated vigorously using ultrasonic agitation at room temperature during this procedure. The dispersion medium was then supplemented with 15 ml more of a 25 percent glutaraldehyde solution, and the mixture was agitated for a further 5 hours. The Chitosan-coated magnetic iron oxide nanoparticles were then extracted from the reaction mixture using a strong external magnetic field created by a permanent magnet. The products were then washed with ethanol and dried for three hours in a vacuum oven at 80°C.

Curcumin drug loading test conducted by in vitro method:

Chitosan-coated magnetic Fe_3O_4 nanoparticles were overloaded with the drug Curcumin (CS). In order to improve the uptake of curcumin, 0.1 percent curcumin solution was loaded with 0.3 gram of magnetic Fe_3O_4 nanoparticles coated with Chitosan (CS-Fe_3O_4) and swirled for 3 hours. The nanoparticles were removed from the mixture at the appropriate time interval. To ascertain the drug content of curcumin, the absorbance of curcumin in the supernatant was measured at max = 428 nm using UV-Vis spectrophotometer. The variation in Curcumin concentration is observed between the initial concentration and the final concentration with a time duration.

Bare and Chitosan Magnetic Composite Characterization

The synthesized composite was characterized using X-Ray Diffraction (XRD), Fourier Transform Infrared Spectroscopy (FTIR), and Scanning Electron Microscopy (SEM) techniques. By using the XRD method, the crystal structures of the produced magnetic composites were analyzed. Using FTIR techniques, the chemical groups and interactions present in the synthesized magnetic composites were located. SEM images were used to determine the sizes and forms of the magnetic composites.

Radiation Diffraction (XRD)

The phase identification of crystal materials and information on the average size of nanocrystals are both done via X-Ray Diffraction. To further understand the crystal structure of the generated bare and Chitosan-coated Fe_3O_4 composite, XRD (Rigaku Ultima-IV X-Ray Diffractometer) was used.

Fourier Transform Infrared Spectroscopy(FTIR)

The chemical makeup of the bare, Chitosan-coatedand Curcumin-loaded Chitosan-coated magnetic composites were studied using Fourier Transform Infrared Spectroscopy. To create pellets, 0.2 g of sample was compressed with 0.18 g of KBr. The FTIR equipment was used to analyze these pellets (Thermo Scientific, Nicolet 6700)

Scanning Electron Microscopy (SEM)

The surface of a sample is scanned line by line using scanning electron microscopes, which provide details about the surface topography and composition of the sample. To see the surface characteristics and size dispersion of the synthetic composite, SEM pictures of the composite in both its naked and Chitosan-coated states were acquired.

Thermal Gravimetric Analysis – Differential Thermal Analysis (TGA-DTA):

A collection of methods known as "thermal analysis" involve measuring a system's physical or chemical quality as a function of temperature. All materials incur physical and chemical changes as a result of temperature fluctuations. A suitable transducer can be used to detect the changes, and the electrical signals they produce are then collected and analyzed to create thermograms, which demonstrate how a property changes as a function of temperature. A Mettler TA3000 thermal analyzer was used to perform a thermogravimetric analysis (TGA) with a sample weight of 3-5 mg and a heating rate of 5°C min-1 in a nitrogen atmosphere.

Vibrating Sample Magnetometer (VSM)

Magnetization as a function of applied field at room temperature (M-H curve) wasmeasured for all the samples using a commercial VSM. The magnetic fieldcan vary up to ±12 kGauss. In another way, magnetization is measured as a functionof temperature at a constant magnetic field.

Temperature can be varied from 30K to room temperature. The VSM operates on the principle of Faraday'slaw of induction, i.e., that a changing magnetic field will produce an electric field (Foner, 1996). This electric field can be measured, which in turn can provide us with informationabout the magnetic moment of the sample as the magnetic field is varied.

The sample is fixed to the lower end of the quartz sampleholder. The measurement sequence is then programmed using the software providedwith the instrument. The vibration exciter is then started, and the signal received fromthe probe and the pickup coils is converted into the magnetic moment value of thesample. The M-H curve gives the information about the saturation magnetization (inemu/g), magnetic coercivity (in Oe), remanence magnetization (in emu/g) and magneto crystalline anisotropy constant (Keff).

Procedure for Anti-Microbial analysis:

For a given anti–microbial agent, there is an approximate linear relationship between the logarithm of the M.I.C. and the zone diameter for organisms with reasonably comparable growth rates. Using their own standardized technique, Bauer et al. (1966)studies have correlated zone diameters of multiple anti–microbial agents with M.I.C.'s as determined by tube and agar dilution methods.

Preliminary analysis of anti–microbial activity was conducted by using the agar well diffusion assay. For fungal samples, the inoculum was prepared in Sabour aud Dextrose Broth (SDB) solution and incubated for 4 hours. Then 0.1 ml of the inoculum was homogeneously inoculated on Petri plates containing SDA (Hi-Media Labs Ltd.) medium, then wells of 6 mm diameter were punctured on it by using sterile cork–borer. A 50 µl of biologically synthesize nanoparticles was loaded in the wells using sterilized micropipettes.

Sterile SDB water was used as a negative control. Plates were incubated for 24–48 hours at 25°C. A zone of Inhibition in mm was determined.

For bacterial cultures, the inoculum was prepared in peptone broth and incubated for 4 hours. Then 0.1 ml of the inoculum was homogeneously inoculated on Petri–plates containingMuller–Hinton (MH) agar (Hi-Media Labs Ltd.) medium. Wells of 6 mm diameter were punctured on it by using sterile cork–borer and 50 µl of biologically synthesize silver nanoparticles were poured in the wells using sterilized micropipettes. Plates were incubated for 18–24 hours at 37°C. A zone of Inhibition in mm was determined. The disc diffusion method of anti–microbial susceptibility should be regarded, therefore, as a reproducible semi–quantitative estimation of the M.I.C. for fast growing organisms if the standardized methodology is rigorously followed.

Results and Discussion

Steps in the formation of Fe_3O_4 nanoparticles

In the study, ex-situ co-precipitation was used to create nanoparticles supported biomaterial made of Chitosan and iron oxide as a potential drug delivery system. Due to the straightforward and moderate synthesis conditions, co-precipitation approach, according to Unsoy et al. (2014), may be a very beneficial way to synthesize nanoparticles for biomedical use. Additionally, co-precipitated nanoparticles exhibit greater biocompatibility and biodegradability. Nanoparticles' physical properties and magnetic traits were impacted by a number of variables, including composition ratio and crosslinking duration. By adding base solution continually while synthesizing Fe_3O_4, the colour of the iron solution gradually changed from light brown to dark brown and then to black. Fe_3O_4 nanoparticle production was indicated by the development of a dark precipitant. The compund generated throughout the synthesis steps, changed in phases, which is why the colour of the sample changed.

FTIR

Figure 1.1 displays the FT-IR spectra of iron oxide. In this result various wavelength peaks are identified. The peaks are indicated the results of the presence of peaks at wavelengths of 462.56, 581.85, 881.37, 1060.40, 1156.06, 1353.32, 1603.50, 1630.09, 1719.75, 1793.75, 2922.84 and 3460.97 cm^{-1}. Of these peaks, the 1719.75, 1793.75, 2922.84 and 3460.97 cm-1 was very sharp and broad compared to the other peaks indicating the high concentration at these regions. The peak at 3460.97 is stretching vibrations of O-H. The peak 2922.84 stretching of N-H group and the peaks of 1793.75 and 1719.75 peaks are stretching of C=O groups. The peaks of 1630.09 and 1603.50 are represents the C=C.

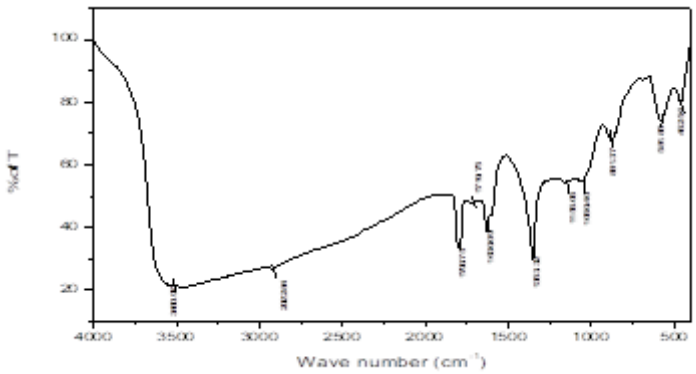

Figure1.1: FT-IR spectra of iron oxide

Figure 1.2 shows the FT-IR spectra of iron oxide/chitosan nanoparticle. In the results, the different wavelengths were noticed. The obtained wavelengths were 3475. 99, 2921.40, 1805.40, 1790.15, 1723.76, 1629.12, 1602.82, 1351.20, 1153.11, 1061.98, 879.02, 552.48, 464.89 and 458.11cm^{-1}. The peaks of 3475. 99 represents the strong bonding of O-H,

2921.41 and 1805.40 indicates the C-H bonding, 1790.15 and 1723.76 represents the C-O strong bonding 1629.12 and 1602.82 indicates C=C bonding and 1351.20 represents the O-H bonding. The presence of an extra peak at 464.89 and 458.11 cm^{-1}, attributable to the Fe-O group in addition to the typical Chitosan peaks, shows that iron oxide nanoparticles were successfully incorporated into the Chitosan particles.

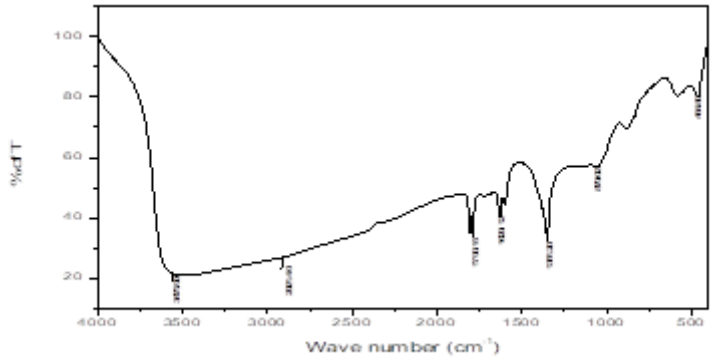

Figure 1.2: FT-IR spectra ofiron oxide/CS

Figure 1.3 shows the FT-IR spectra of iron oxide/chitosan/curcumin loaded nanoparticle. The results obtained at 3444.81, 2923.88, 1805.30, 1790.11, 1768.87, 1732.78, 1351.20, 1050.50, 880.51, 853.96, 694.17, 583.49 and 458.44 cm^{-1}. The peaks of 3444.81 represents the strong bonding of O-H, 2923.88 and 1805.30 represents the C-H bonding, 1790.11, 1768.87 and 1732.78 wavelengths represents the C=O bonding and 1351.20 represents the O-H bonding. The CS-iron oxide composites' weaker peaks at 1000–1100 cm^{-1} in comparison to CS–iron oxide suggested that Curcumin had been added to the material. While the FT-IR diagram of the curcumin/CS-iron oxide composites demonstrated how the surface of the composites was altered by small groups following curcumin alterations.

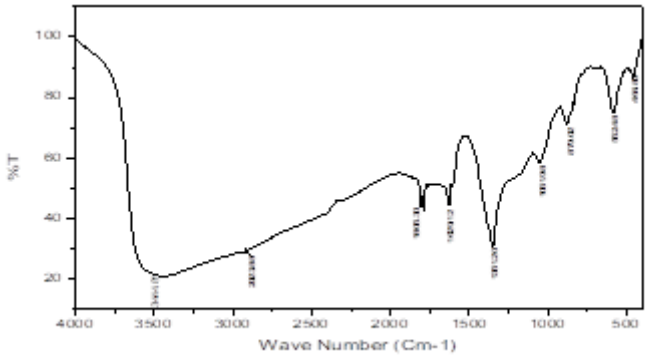

Figure 1.3: FT-IR spectra of Curcumin loaded CS-Iron Oxide

XRD

The XRD examination (Fig. 2), which displays the distinctive magnetite diffraction peaks at 2θ = 44.43° and 64.10° and is consistent with JCPDS Card No. 96-900-2327, confirmed the crystal structure. The outcomes demonstrated that the iron oxide was successfully immobilized, or blended. The significant amorphous phase of Chitosan was present. The biomaterial displayed a diffraction pattern that was similar to that of CS-iron oxide after being modified with curcumin. The iron oxide peak intensity was shown to have significantly increased with the gradual increment on the curcumin/CS-iron oxide curve.The XRD data confirmed that the iron oxide nanoparticles were crystalline in nature as the values matched well with the standard reference of the Joint Committee on Powder Diffraction Standards of iron oxide nanoparticles. The sharp and clearly visible peaks of XRD profile

confirmed that the particles were crystalline. The iron oxide peaks was increased in all the structure. The similar increase in the strength of the distinctive iron oxide peaks was also noted in studies of Bajpai et al (2013).

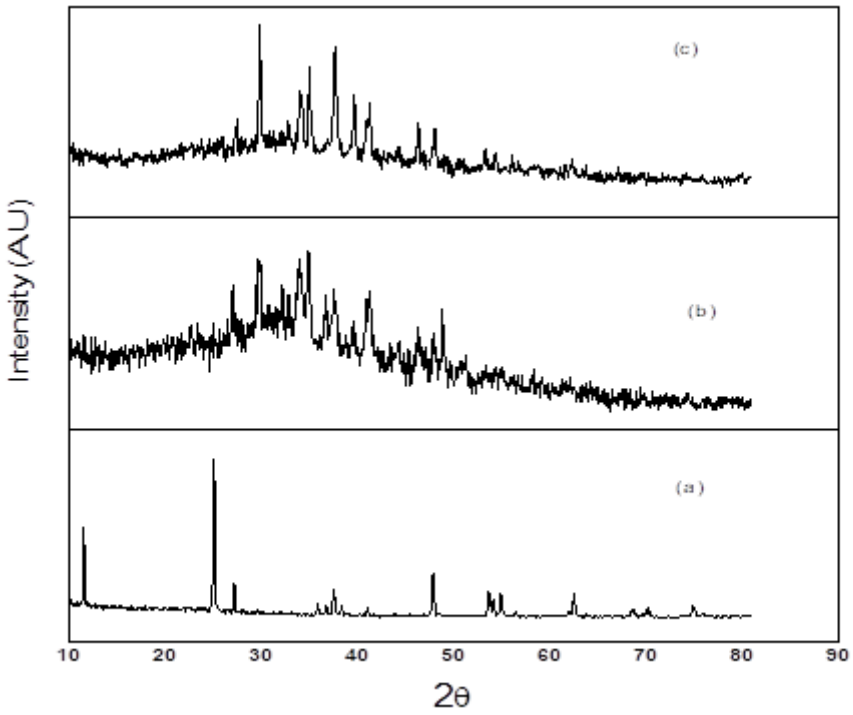

Figure 2 (c): XRD analysis of a) Iron oxide Nano particles b) CS- Iron oxide Nano particles c)Curcumin/CS-ironoxide nanoparticle

SEM

Figures 3.1 and 3.2 show SEM images of the produced CS-ironoxide and Curcumin/CS-ironoxide particles. Images of curcumin/CS-ironoxide demonstrate that Fe_3O_4has a polydisperse size distribution. As opposed to Curcumin/CS-ironoxide, CS-ironoxide has a monodisperse size dispersion and is smaller in size (Figure 3.1 and 3.2).

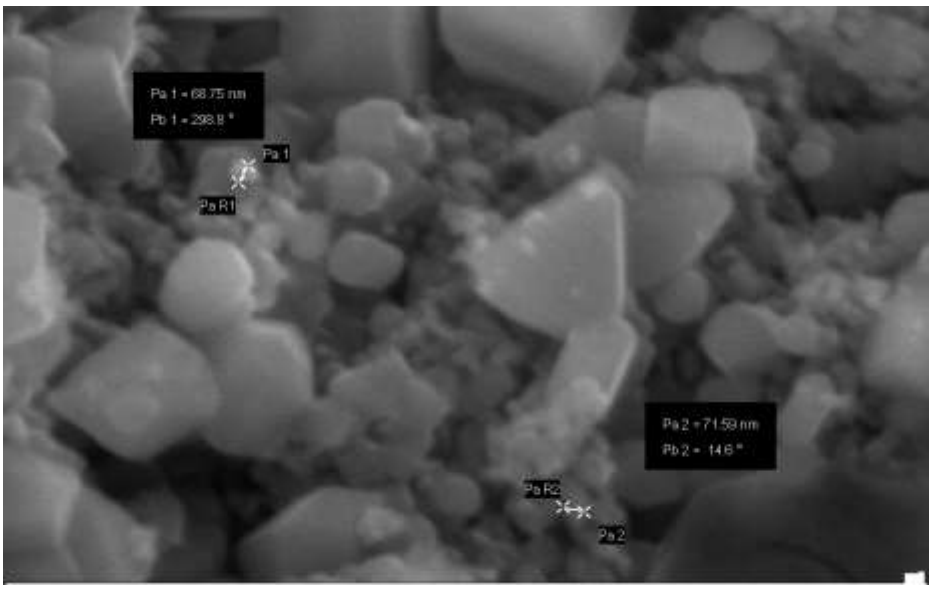

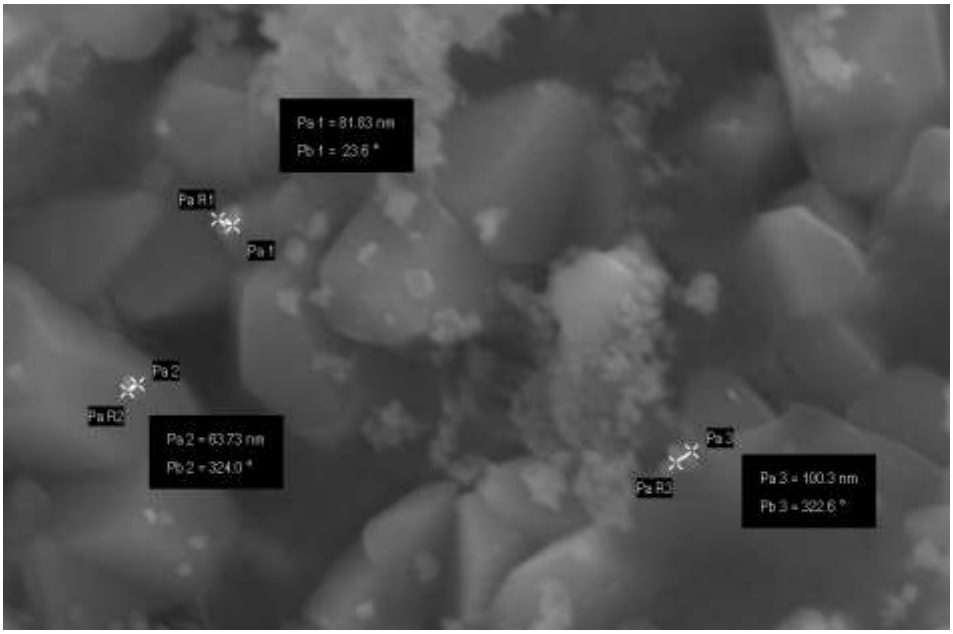

Figure 3.1 and Figure 3.2: SEM images of CS-ironoxide and Curcumin/CS-ironoxide particles

UV–Vis

The observed color change and single peak absorbance spectra were caused by distinctive vibrations brought on by changes in the metal nanoparticles electrical energy levels. The absorbance scan by UV-Vis spectrophotometer of the synthesized Curcumin/CS-Fe_3O_4nanoparticles revealed a prominent plasmon peak (Figure 4) and confirmed the range of Fe_3O_4 in the nano-scale. The Fe_3O_4nanocrystallites had a peak in the 280–470 nm wavelength range. The magnitude, peak, and width of the spectrum band are affected by the characteristics of the nanomaterial such as its size, shape, and distribution.

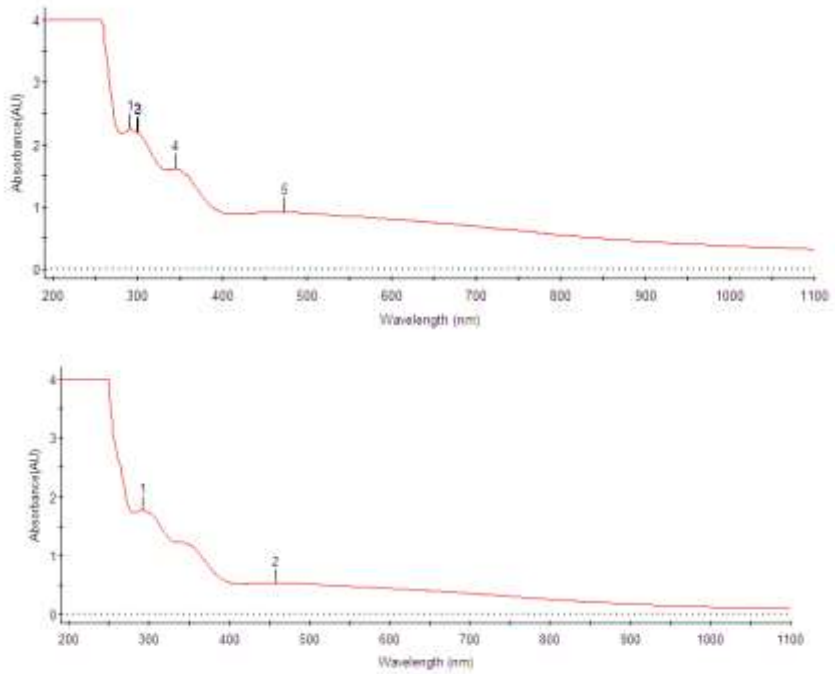

Fig:4.1 and Fig:4.2: Showing the graphical representation of UV–spectroscopy results for the CS-ironoxide and Curcumin/CS-ironoxide

TGA-DTA Analysis

This technique is used to find the thermal stability of the nanomaterials. In this techniques find the weight loss at the increasing temperature at a constant rate (Rajisha et al., 2011). The lifetime of nanomaterials are easily identified by using this technique.

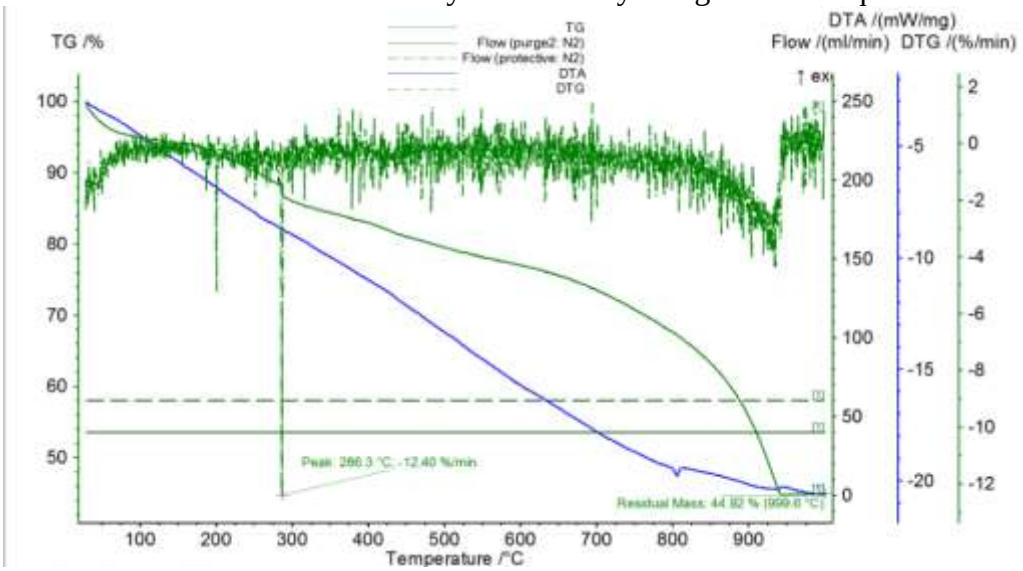

Figure 5: TGA-DTA analysis of Iron Oxide/chitosan/curcumin nanoparticle

Thernal analysis is a vital technique to find the composition of as-prepared ironoxide nanoparticles and their thermal stability. The thermal behavior of ironoxide nanoparticles was elucidated using TGA and DTA analysis (Figure 5). The finding results proved that the ironoxide/chitosan/curcumin nanoparticles have two mass loss steps in the temperature ranges in 200 and 250-300^{0}C respectively. The TGA curve, the first step is attributed to the removal of hygroscopic water molecule. The second step is mostly related to the condensation of molecules and the evaporation of water molecules.

VSM ANALYSIS

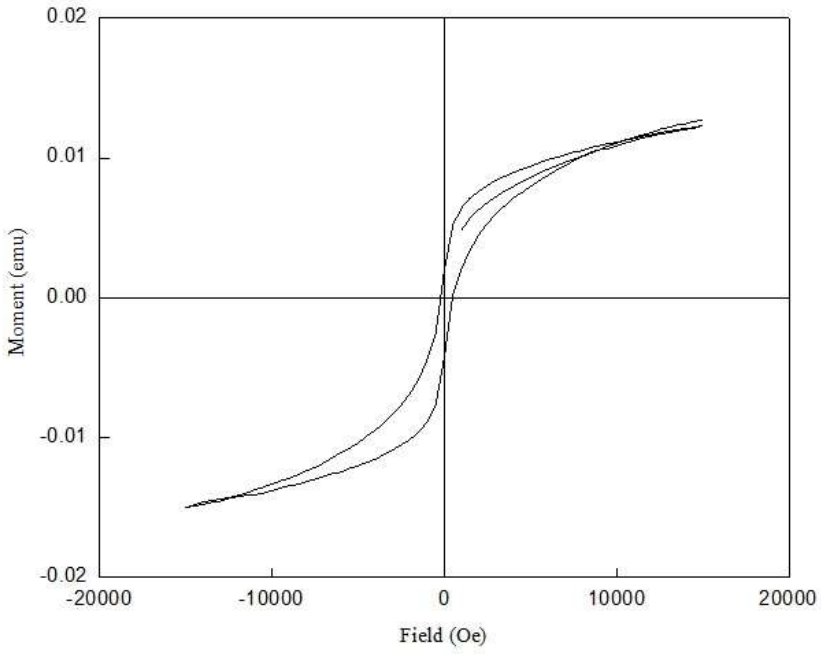

Figure 6: VSM analysis for ironoxide/chitosan/curcumin nanoparticle

Static magnetization curves were recorded in a vibrating sample magnetometer. The VSM measurements of clustered MNPs were carried out at a particular temperature in the applied magnetic field sweeping from −0.02 to 0.02 T. The result measures the saturation magnetization and the magnetic moments were measured.

The synthesized nanoparticles magnetization nature was analysed at normal room temperature 37ºC. The previous study of Sushmitha et al., (2021) proves that the saturation magnetization of iron oxide nanoparticle is 55.83 emu/g. Suggesting that they have strong magnetic properties. In the present study, proved that the magnetization values of chitosan/ironoxide/curcumin is 13.824 emu/g is obtained with VSM analyses. A decrease was observed in the magnetization values owing to the decreased core sizes of magnetites incorporated in the chitosan-coating.

The magnetic field is relaxed in the prepared iron oxide nanoparticles, the magnetization decreases from plateau to zero state **(**El-Boubbou et al., 2009). The similar effect is noted in the present study also. This effect clearly proves the super paramagnetic behaviour of nanoparticles. In the absence of a magnetic field the superparamagnetic does not shows the magnetic properties.

The biopolymers is used to increases the magnetic nature of the super paramagnetic nanoparticles. Biopolymer coated nanoparticles are effectively used for imaging, diagnosis purposes and treatment purpose due to magnetic nature it can be actively targeted in mangnetic field and it have the large surface to volume ratio (Yezhelyev et al., 2006; Pison et al., 2006).

Anti-microbial activity of ironoxide, ironoxide-CS and ironoxide-CS-curcumin coated nanoparticle

The anti–microbial activities of ironoxide/chitosan/curcumin nanoparticles were studied by using the agar well diffusion method. For this purpose, gram positive and gram negative bacteria E. coli, Staphylococcus and Klebsiella pneumonia strains were used. Staphylococcus strains were used as model gram positive bacteria and E. Coli and Klebsiella pneumonia as a gram negative bacteria.

Table 1, 2 and 3 have shown the results of anti–bacterial properties of iron oxide, iron oxide/chitosan and ironoxide/chitosan/curcumin coated nanoparticle. From the table, it is clear that the anti–bacterial activities of synthesized nanoparticles, are higher that of their respective control of gentamicin antibiotic disc. This is due to the smaller size and high surface to volume ratio of nanoparticles, which enables them to interact closely with the microbial membrane.

Table 1: The anti–microbial activities of ironoxide for the gram positive and gram negative bacteria ofStaphylococcus,E. Coli and Klebsiella pneumoniastrains

SAMPLE	Zone of inhibition (mm/ml)				
	25 µl	**50 µl**	**75 µl**	**100 µl**	**Control**
Staphylococcus	08	13	15	18	22
E.coli	06	11	12	15	20
Kleb	04	10	12	17	18

Table 2: The anti–microbial activities of ironoxide-chitosan for the gram positive and gram negative bacteria of Staphylococcus, E. coliand Klebsiella pneumoniastrains

SAMPLE	Zone of inhibition (mm/ml)				
	25 µl	**50 µl**	**75 µl**	**100 µl**	**Control**
Staphylococcus	09	12	15	20	20
E.coli	08	10	15	18	18
Kleb	07	10	13	14	18

Table 3: The anti–microbial activities of ironoxide-chitosan-curcumin loaded for the gram positive and gram negative bacteria of Staphylococcus, E. coliand Klebsiella pneumoniastrains

SAMPLE	Zone of inhibition (mm/ml)				
	25 µl	**50 µl**	**75 µl**	**100 µl**	**Control**
Staphylococcus	09	15	18	23	22
E.coli	07	14	17	20	20
Kleb	06	13	16	17	18

The zone of inhibition is higher in the case of gram negative bacteria than gram positive bacteria.This is due to the accumulation of large number of peptidoglycan layers on the walls of gram positive bacteria compared to gram negative bacteria. This peptidoglycan layer prevents the nanoparticles from entering the cytoplasmic membrane than gram negative bacteria. Hence, the present study highlights that the synthesized nanoparticles can effectively control the microorganism and to prevent the harmful infections.Prabhuet al. (2010) have detailed that the positive charge on the silver particle is pivotal for its anti–microbial activity through electrostatic attraction between the negative charge on the cell membrane of the microorganism and positively charged nanoparticles.

Consequently, this effortless approach for producing the ironoxide, chitosan and curcumin coated nanoparticles produces valuable in many industrial applications. The method authorizes the use of a nontoxic, inexpensive, ecofriendly and bioavailable material. Faizan Abul Qais et al. (2019) synthesis the nanoparitcles using the extracts of Murrayakoenigii. These nanoparticles effectively inhibited the growth of various pathogens. This may prove in the present study also.

Conclusion

The current research effort has been effective in creating brand-new Chitosan-iron oxide nano-composites with curcumin. The characteristics of the produced nano-composites' and the possible uses have been carefully examined. Because of its antibacterial, antifungal and antioxidant characteristics, Chitosan offers a variety of biomedical applications on its own. The characteristics of Chitosan nano-composites changed and improved when they were

combined with iron oxide nanoparticles and Curcumin. Some further studies are needed an in vivo models. Hence, it may be used as a potent drug in near future.

REFERENCES

[1] Hariani, P.L., Faizal, M., Ridwan, Marsi and Setiabudidaya, D. (2013). Synthesis and Properties of Fe_3O_4 Nanoparticles by Co-precipitation Method to Removal ProcionDye.International Journal of Environmental Science and Development. 4: 336-34.

[2] Mahdavi, M., Ahmad, M., Haron, M.J., Namvar, F., Nadi, B., AbRahman, M.Z. and Amin, J. (2013). Synthesis, Surface Modification and Characterisation of Biocompatible Magnetic Iron Oxide Nanoparticles for Biomedical Applications.Molecules. 18: 7533-7548.

[3] Wu, W., He, Q. and Jiang, C. (2008). Magnetic iron oxide nanoparticles: synthesis and surface functionalization strategies. NanoscaleResLett. 3: 397–415.

[4] Bauer, A.W., Kirby, W.M., Sherris, J.C. and Turck. M. (1966).Antibiotic susceptibility testing by a standardized single disk method. Am J Clin Pathol.45(4):493-496.

[5] Unsoy, G., Khodadust, R., Yalcin, S., Mutlu, P. and Gunduz, U. (2014). Synthesis of Doxorubicin Loaded Magnetic Chitosan Nanoparticles for pH Responsive Targeted Drug Delivery.European Journal of Pharmaceutical Science. 62: 243-250.

[6] Ibezim, E.C., Andrade, C.T., Marcia, C., Baretto, B., Odimegwu, D.C. and De Lima, F.F. (2011). Ionically Cross-linked Chitosan/Tripolyphosphate Microparticles for the Controlled Delivery of Pyrimethamine Ibnosina. Journal of Medicine and Biomedical Sciences. 3: 77-88.

[7] Muzzarelli, R.A., Mattioli-Belmonte, M., Pugnaloni, A. and Biagini.(1999). Biochemistry, histology and clinical uses of Chitins and Chitosans in wound healing.EXS. 87: 251–264.

[8] Crini, G., Gimbert, F., Robert, C., Martel, B., Adam, O., Crini, N.M., Giorgi, F.D. and Badot, P.M. (2008). The removal of Basic Blue 3 from aqueous solutions by Chitosan-based adsorbent: Batch studies. Journal of Hazardous Materials.153: 96-106.

[9] Hua, L.L., Cheng, J.D., Deng, H.R., Liu, Z.L. and Li, X.L. (2010). Preparation, characterization and antimicrobial activities of chitosan/Ag/ZnO blend films. Chem. Eng. J. 160: 378-382.

[10] Thacharodi, D. and Panduranga, R.K. (1993). Propranolol hydrochloride release behaviour of crosslinked chitosan membranes. Journalof Chem. Technol. Biotechnol.58: 177-181.

[11] Thacharodi, D. and Panduranga, R.K. (1993).Release of nifedipine through crosslinked chitosan membranes.Int. J. Pharm. 96: 33-36.

[12] Thacharodi, D. and Panduranga, R.K. (1995). Development and in vitro evaluation of citosan-based transdermal drug delivery systems for the controlled delivery of propranolol hydrochloride.Biomaterials. 16: 145-148.

[13] Chen, W., Shen, H.B., Li, X.Y., Jia, N.Q. and Xu, J.M. (2006). Synthesis of immunomagnetic nanoparticles and their application in the separation and purification of $CD34^+$ hematopoietic stem cells.Appl. Surf. Sci. 253: 1762-1769.

[14] Bajpai, A.K. and Sweta Likhitkar. (2013). Investigation of magnetically enhanced swelling behaviour of superparamagnetic starch nanoparticles. Bull. Mater. Sci. 36(1): 15–24.

[15] Rajisha., K.R., Deepa, B., Pothan. L.A. and Thomas, S. (2011). 9-Thermomechanical and Spectroscopic characterization of natural fibre composites. Woodhead Publishing series in Composites Science and Engineering. 241-274.

[16] Shen, H.B., Long, D.H., Zhu, L.Z., Li, X.Y., Dong, Y.M., Jia, N.Q., Zhou, H.Q., Xin, X. and Sun, Y. (2006). Magnetic force microscopy analysis of apoptosis of HL-60 cells induced by complex of antisense nucleotides and magnetic nanoparticles.Biophys. Chem. 122: 1-4.

[17] Liu, X., Xing, J., Guan, Y., Shan, G. and Liu, H. (2004). Synthesis of amino-silane modified superparamagnetic silica supports and their use for protein immobilization. Colloids Surf. A Physicochem.Eng. Asp. 238: 127–131.

[18] Laurent, S., Forge, D., Port, M., Roch, A., Robic, C., Vander, E.L. and Muller, R.N. (2008). Magnetic iron oxide nanoparticles: synthesis, stabilization, vectorization, physicochemical characterizations, and biological applications.Chem. Rev. 108: 2064-2110.

[19] Yoon, T.J., Kim, J.S., Kim, B.G., Yu, K.N., Cho, M.H. and Lee, J.K. (2005). Multifunctional nanoparticles possessing a "magnetic motor effect" for drug or gene deliveryAngew.Chem. Int. Ed. 44: 1068-1071.

[20] Kawamori, T., Lubet, R., Steele, V.E., Kelloff, G.J., Kaskey, R.B., Rao, C.V. and Reddy, B.S. (1999). Chemopreventive effect of Curcumin, a naturally occurring anti-inflammatory agent, during the promotion/progression stages of colon cancer. Cancer Res. 59(3): 597-601.

[21] Mahady, G.B., Pendland, S.L., Yun, G. and Lu, Z.Z. (2002). Turmeric (Curcuma longa) and Curcumin inhibit the growth of Helicobacter pylori, a group 1 carcinogen. Anticancer Res. 22: 4179-4181.

[22] Agarwal, B.B., Sundaram, C., Malani, N., Ichikawa, H., Aggarwal, B.B., Surh, Y.J. and Shishodia, S.(2007). The Molecular Targets and Therapeutic Uses of Curcumin in Health and Disease (New York: Springer) pp 1–76.

[23] Prabhu Nagarajan., Divya T. Raj., K. Yamuna Gowri. and Ayisha Siddiqua, S. (2010). Synthesis of silver phyto nanoparticles and their antibacterial efficacy. Digest Journal of Nanomaterials and Biostructures 5(1):185-189.

[24] SushmithaLakshminarayanan, M. Furhana Shereen, K. L. Niraimathi, P. Brindha & A. Arumugam. (2021). One-pot green synthesis of iron oxide nanoparticles from Bauhinia tomentosa: Characterization and application towards synthesis of 1, 3 diolein. Nature. Scientific Reports. 11; 8643.

[25] El-Boubbou, K. et al.(2019). Preparation of iron oxide mesoporous magnetic microparticles as novel multidrug carriers for synergistic anticancer therapy and deep tumor penetration. Sci. Rep. 9, 1–20.

[26] Patwa, R., Zandraa, O., Capáková, Z., Saha, N. &Sáha, P. (2020). Effect of iron-oxide nanoparticles impregnated bacterial cellulose on overall properties of alginate/casein hydrogels: Potential injectable biomaterial for wound healing applications. Polymers (Basel). 12, 1–21.

[27] Yezhelyev, M. V., Gao, X., Xing, Y., Al-Hajj, A., Nie, S. and O'Regan, R. M. (2006). Emerging use of compositein diagnosis and treatment of breast cancer. The Lancet Oncology, 7(8); 657-667.

[28] Pison, U., Welte, T., Giersig, M. and Groneberg, D.A. (2006). Nanomedicine for respiratory diseases. European Journal of Pharmacology. 533(1); 341-350.

[29] Faizan Abul Qais., Anam Shafiq., Haris M. Khan., Fohad M. Husain., Rais A. Khan., Bader Alenazi., Ali Alsalme. and Iqbal Ahmad. (2019).Synthesized Using Murrayakoenigii (L.) against Multidrug-Resistant Pathogens. Bioinorganic Chemistry and Applications. Article ID 4649506 | https://doi.org/10.1155/2019/4649506.